Journal of Power Sources 238 (2013) 296–300

Contents lists available at SciVerse ScienceDirect

Journal of Power Sources

journal homepage: www.elsevier.com/locate/jpowsour

Short communication

NaFSA–C_1C_3pyrFSA ionic liquids for sodium secondary battery operating over a wide temperature range

Changsheng Ding [a], Toshiyuki Nohira [a,*], Keisuke Kuroda [a], Rika Hagiwara [a,*], Atsushi Fukunaga [a,b], Shoichiro Sakai [b], Koji Nitta [b], Shinji Inazawa [b]

[a] Graduate School of Energy Science, Kyoto University, Sakyo-ku, Kyoto 606-8501, Japan
[b] Electronics & Materials R&D Laboratories, Sumitomo Electric Industries, Ltd., Konohana-ku, Osaka 554-0024, Japan

HIGHLIGHTS

- The physicochemical properties of NaFSA–C_1C_3pyrFSA ionic liquids were evaluated.
- The conductivity is 15.6 mS cm^{-1} at 353 K for the melt containing 20 mol% NaFSA.
- The electrochemical window of this ionic liquid is as wide as 5.2 V at 353 K.
- The cell using $NaCrO_2$ positive electrode exhibits stable ch.–disch. behaviour at 298 and 353 K.
- The cell also shows high discharge rates, reaching 500 mA g^{-1} at 353 K.

ARTICLE INFO

Article history:
Received 13 January 2013
Received in revised form
3 March 2013
Accepted 7 March 2013
Available online 26 March 2013

Keywords:
Sodium secondary battery
Ionic liquid
N-Methyl-*N*-propylpyrrolidinium
Bis(fluorosulfonyl)amide
$NaCrO_2$

ABSTRACT

The physicochemical properties of NaFSA–C_1C_3pyrFSA ionic liquids were investigated to explore their potential as new electrolytes for sodium secondary batteries operating over a wide temperature range. The viscosity and ionic conductivity of NaFSA–C_1C_3pyrFSA with a molar ratio of 2:8 were 16.7 cP and 15.6 mS cm^{-1}, respectively, at 353 K. The electrochemical window of this ionic liquid was 5.2 V at 353 K with sodium metal deposition determining the cathode limit. A Na/NaFSA–C_1C_3pyrFSA/$NaCrO_2$ cell exhibited stable charge–discharge behaviour at 298 and 353 K. The discharge capacities of 92 and 106 mAh $(g\text{-}NaCrO_2)^{-1}$ were observed at 298 and 353 K, respectively, at 20 mA g^{-1}. The Coulombic efficiency was higher than 99% during the charge–discharge tests except for the initial few cycles. The cell also showed high discharge rates, reaching 500 mA g^{-1} at 353 K.

1. Introduction

Electricity generated from renewable sources such as solar and wind power offers enormous potential for meeting future energy demands. However, solar and wind energy supplies are only intermittent, whereas electricity must be reliably available for 24 h a day. Therefore, energy storage systems are required for the effective use of renewable energy sources, i.e., to store energy until needed by the electrical grid. Lithium ion batteries, the most common type of secondary batteries found in almost all portable electronic devices, are a possible solution to this issue [1]. There is an increasing demand for lithium ion batteries as a major power source in portable electronic devices and vehicles. However, current lithium ion batteries have several problems affecting their application as large-scale storage devices. First, the use of volatile and flammable organic electrolytes is a significant disadvantage in realizing safe batteries. This hinders the development of large-scale batteries possessing high energy and power density. Moreover, the future global supply of high-quality lithium itself is uncertain.

Sodium secondary batteries are attracting much attention for energy storage applications and have been studied for a long time. This is because of the advantages of sodium, notably its low cost, high abundance, low toxicity, and reasonably high energy density [2–19]. Among the many types of sodium secondary batteries, Na/S [2,3] and Na/$NiCl_2$ [4,5] batteries have been applied in practice. However, high operation temperatures (523–573 K) are required

* Corresponding authors. Tel.: +81 75 753 5822; fax: +81 75 753 5906.
E-mail addresses: nohira@energy.kyoto-u.ac.jp (T. Nohira), hagiwara@energy.kyoto-u.ac.jp (R. Hagiwara).

0378-7753/$ – see front matter © 2013 Elsevier B.V. All rights reserved.
http://dx.doi.org/10.1016/j.jpowsour.2013.03.089

because the solid β″-alumina electrolyte exhibits high ionic conductivity only at high temperatures. Moreover, handling these batteries can be difficult because of the brittleness of β″-alumina, especially during heating and cooling operations. The high operation temperatures also result in an increase in the size, weight, and cost of the batteries. Thus, it is important to develop sodium secondary batteries without using β″-alumina as an electrolyte so that they can be operated at lower temperatures. In the last few years, sodium secondary batteries operating at room temperature have also been reported [6–19]. However, the cyclability and charge–discharge rates of the reported room-temperature sodium secondary batteries are still lower as compared with those of the current lithium ion batteries. Moreover, the reported room temperature sodium secondary batteries use usually organic electrolytes such as $NaClO_4$/propylene carbonate, which are disadvantageous for the construction of large-scale safe batteries. Therefore, it is necessary to develop new batteries with better performance and increased safety.

Ionic liquids generally provide negligibly low volatility, nonflammability, and high thermal and electrochemical stability. Consequently, they have been studied and used as safe electrolytes in many electrochemical fields. We have reported that NaTFSA–CsTFSA (TFSA = bis(trifluoromethylsulfonyl)amide) [20] and NaFSA–KFSA (FSA = bis(fluorosulfonyl)amide) [21] ionic liquids are promising electrolytes for sodium secondary batteries operating at intermediate temperatures. A $NaCrO_2$ positive electrode was successfully operated in NaTFSA–CsTFSA ionic liquid at 423 K, and showed a discharge capacity of 83.0 mAh (g-$NaCrO_2$)$^{-1}$ at 10 mA g^{-1} [20]. A Na/NaFSA–KFSA/$NaCrO_2$ cell exhibited a discharge capacity of 77.3 mAh (g-$NaCrO_2$)$^{-1}$ at 15 mA g^{-1}, at 353 K [21]. However, these ionic liquids have rather high melting points (390 K for NaTFSA–CsTFSA and 330 K for NaFSA–KFSA), which limits the operation temperature of the battery. Thus, in order to increase the operation temperature range, new ionic liquids with lower melting points are expected to be developed.

Consequently, we focused on ionic liquid mixtures of NaFSA and C_1C_3pyrFSA (C_1C_3pyr = *N*-methyl-*N*-propylpyrrolidinium). It has been reported that C_1C_3pyrFSA has a low melting point (264 K), high conductivity (6.4 mS cm^{-1} at 298 K), high thermal stability (up to 398 K), and a wide electrochemical window (ca. 5.3 V at 298 K) [22]. Several research groups have also reported that C_1C_3pyrFSA [23] and C_1C_4pyrFSA [24] ionic liquids exhibit good properties as the electrolytes for lithium secondary batteries. Therefore, the NaFSA–C_1C_3pyrFSA ionic liquid is expected to have favourable properties as an electrolyte for sodium secondary battery operating over a wide temperature range.

In this study, the viscosity, ionic conductivity, and electrochemical window of the NaFSA–C_1C_3pyrFSA ionic liquid were measured at 298–353 K. A Na/NaFSA–C_1C_3pyrFSA/$NaCrO_2$ cell was constructed, and its charge–discharge properties were investigated at 298 and 353 K. $NaCrO_2$ was selected as an active material for the positive electrode because of its good performance at both room temperature [10] and intermediate temperatures [21]. It has been also reported that $NaCrO_2$ is a fundamentally safe positive electrode material for sodium ion batteries with liquid electrolytes [25].

2. Experimental

NaFSA (Mitsubishi Materials Electronic Chemicals, purity >99.0%) and C_1C_3pyrFSA (Kanto Chemical Co., purity >99.9%) were purchased and dried under vacuum at 333 K for 24 h. NaFSA–C_1C_3pyrFSA ionic liquids were prepared by mixing NaFSA and C_1C_3pyrFSA in molar ratios of 0:10, 1:9, and 2:8 in an argon-filled glove box. The viscosities of the NaFSA–C_1C_3pyrFSA ionic liquids were measured by a viscometer (Brookfield Engineering Laboratories, DV-II + PRO). Their conductivities were measured by electrochemical impedance spectroscopy using a calibrated cell with two platinum plate electrodes and a potentiostat/galvanostat/frequency response analyzer (Ivium Technologies, IviumStat). The cell constant was determined using standard KCl aqueous solution.

Electrochemical measurements were performed with a three-electrode system constructed in a Pyrex® beaker cell. The electrochemical window of the NaFSA–C_1C_3pyrFSA ionic liquid was measured by cyclic voltammetry. Sodium plate was used as the counter and reference electrodes. A nickel plate and a glassy carbon rod (3 mm in diameter) were used as the working electrodes to investigate the cathode and anode limits of the NaFSA–C_1C_3pyrFSA ionic liquid, respectively. The scan rate for the cyclic voltammetry experiments was 10 mV s^{-1}.

Charge–discharge properties of the Na/NaFSA–C_1C_3pyrFSA/$NaCrO_2$ cell were measured by a two-electrode cell. $NaCrO_2$ was prepared by mixing Na_2CO_3 and Cr_2O_3 and calcining at 1123 K for 5 h under Ar flow. The prepared $NaCrO_2$ was then mixed well with acetylene black (Wako Pure Chemical Industries, purity >99.99%) and polytetrafluoroethylene (PTFE; Sigma–Aldrich) at a weight ratio of 80:15:5 using a mortar and pestle. Then, the mixture was pressed onto an aluminium mesh current collector at 300 MPa, and it was used as the positive electrode. The negative electrode was consisted of a sodium metal and a Ni plate current collector. Charge–discharge tests were conducted at constant current rates of 20, 50, 100, 200 and 500 mA g^{-1} at 353 K and 20 mA g^{-1} at 298 K.

3. Results and discussion

The viscosities of NaFSA–C_1C_3pyrFSA with molar ratios of 1:9 and 2:8 and C_1C_3pyrFSA (denoted as 0:10) at 298–353 K are shown in Fig. 1. The viscosity of the NaFSA–C_1C_3pyrFSA ionic liquid decreases with an increase in temperature. The viscosities of the NaFSA–C_1C_3pyrFSA ionic liquids with molar ratios of 0:10, 1:9, and 2:8 are 10.2, 12.8, and 16.7 cP, respectively, at 353 K. The viscosity of conventional $NaClO_4$/PC electrolyte at 1 mol dm^{-3} has been reported to be 7–8 cP at 298 K [26], which indicates that $NaClO_4$/PC electrolyte is less viscous than NaFSA–C_1C_3pyrFSA ionic liquid. The viscosity of the NaFSA–C_1C_3pyrFSA ionic liquid increases as the molar ratio of NaFSA is increased.

Fig. 2 shows the ionic conductivities of the NaFSA–C_1C_3pyrFSA ionic liquids with molar ratios of 0:10, 1:9, and 2:8 at 298–353 K. The ionic conductivity of the NaFSA–C_1C_3pyrFSA ionic liquid increases with increasing temperature. The ionic conductivities of the NaFSA–C_1C_3pyrFSA ionic liquids with molar ratios of 0:10, 1:9, and 2:8 are 30.8, 19.8 and 15.6 mS cm^{-1} at 353 K, respectively. The

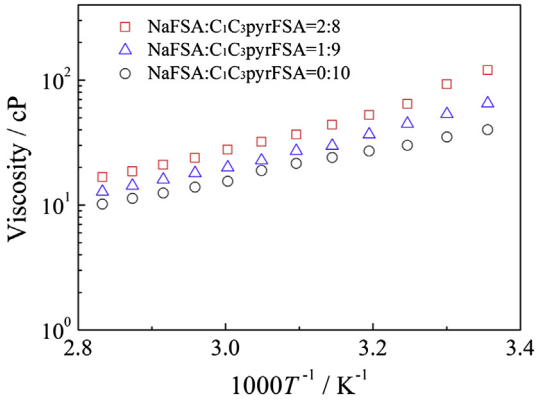

Fig. 1. Temperature dependence of viscosity for NaFSA–C_1C_3pyrFSA ionic liquids with molar ratios of 0:10, 1:9, and 2:8.

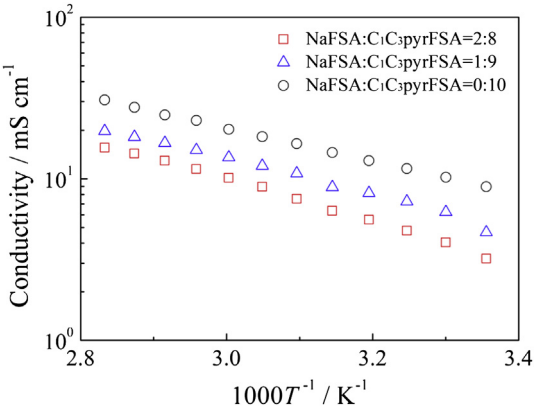

Fig. 2. Temperature dependence of conductivity for NaFSA–C_1C_3pyrFSA ionic liquids with molar ratios of 0:10, 1:9, and 2:8.

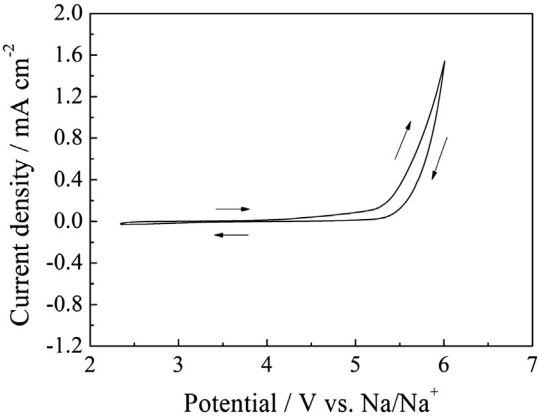

Fig. 4. Cyclic voltammogram (1st cycle) of a glassy carbon rod electrode in NaFSA–C_1C_3pyrFSA ionic liquid at 353 K.

conductivity of conventional $NaClO_4$/PC electrolyte at 1 mol dm^{-3} has been reported to be 5–6 mS cm^{-1} at 298 K [26]. Thus, the conductivities of NaFSA–C_1C_3pyrFSA ionic liquids at 353 K are 3–4 times higher than that of $NaClO_4$/PC at 298 K. It can be also seen that the ionic conductivity of the NaFSA–C_1C_3pyrFSA ionic liquid decreases with increasing molar ratio of NaFSA, because of the increase in viscosity.

When used as an electrolyte, an ionic liquid is expected to have low viscosity and high ionic conductivity. When used in a sodium secondary battery, an ionic liquid should also have a relatively high concentration of Na^+ ions. However, in the NaFSA–C_1C_3pyrFSA ionic liquid, the viscosity increases and the ionic conductivity decreases with increasing Na^+ concentration. Considering that the conductivity of 15.6 mS cm^{-1} is sufficient for the sodium secondary battery applications and that high Na^+ concentrations are desirable, the NaFSA–C_1C_3pyrFSA ionic liquid with a molar ratio of 2:8 was selected as the electrolyte in this study. This ionic liquid has a conductivity of 3.2 mS cm^{-1} even at 298 K.

A cyclic voltammogram (steady cycle) of a nickel electrode in the NaFSA–C_1C_3pyrFSA ionic liquid with a molar ratio of 2:8 at 353 K is shown in Fig. 3. A pair of cathodic and anodic currents is observed at 0 V vs. Na/Na^+, which corresponds to the deposition and dissolution of sodium metal. However, the coulombic efficiency for deposition and dissolution is not high at a nickel electrode, which may be due to the dendrite formation. Meanwhile, a sodium deposition–dissolution cycle test at a current density of 0.5 mA cm^{-2} on a copper electrode at 353 K shows the cycle efficiency of 94% (see Supplementary information), suggesting that the deposition and dissolution occurs reversibly on an appropriate electrode material. Fig. 4 shows a cyclic voltammogram (1st cycle) of the glassy carbon rod electrode in the NaFSA–C_1C_3pyrFSA ionic liquid at 353 K. It can be seen that anodic current increases rapidly from 5.2 V vs. Na/Na^+. The anodic current is believed to correspond to the irreversible oxidation of FSA anions. From the results in Figs. 3 and 4, the electrochemical window of the NaFSA–C_1C_3pyrFSA ionic liquid with a molar ratio of 2:8 is determined to be 5.2 V at 353 K, when the limiting potentials are defined as the potential at a current density of 0.1 mA cm^{-2}. The wide electrochemical window indicates that the NaFSA–C_1C_3pyrFSA ionic liquid is highly desirable as an electrolyte for sodium secondary batteries.

Aluminium was used as a current collector for the cathode in this study. The stability of the aluminium plate electrode was investigated before the charge–discharge tests. Since the highest charging voltage is 3.5 V in the present study, the stability test for the aluminium plate electrode was conducted at 3.8 V vs. Na/Na^+ in the NaFSA–C_1C_3pyrFSA ionic liquid at 353 K. Fig. 5 shows the current–time curve during the stability test. The current is negligibly small, below 0.6 μA cm^{-2}, implying that the aluminium plate electrode is electrochemically stable at potential of 3.8 V vs. Na/Na^+. Moreover, a preliminary test indicates that aluminium is stable even at 5.0 V vs. Na/Na^+. Similar electrochemical stability of aluminium at least 4.5 V vs. Na/Na^+ has been confirmed for NaFSA–KFSA ionic liquid at

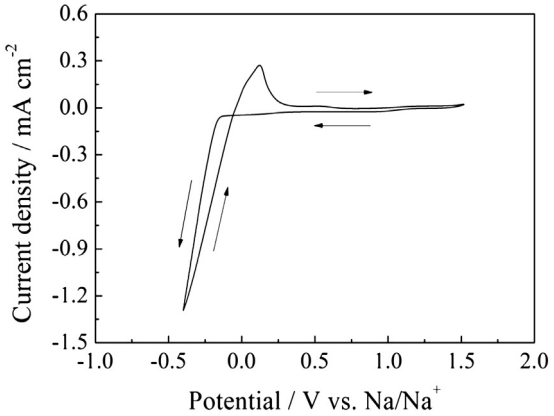

Fig. 3. Cyclic voltammogram (steady cycle) of a Ni plate electrode in NaFSA–C_1C_3pyrFSA ionic liquid at 353 K.

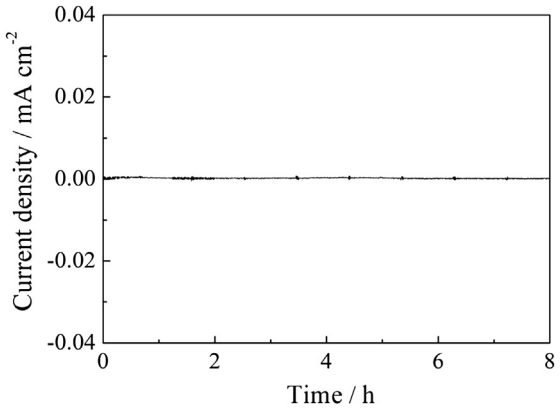

Fig. 5. Chronoamperogram of an Al plate electrode in NaFSA–C_1C_3pyrFSA ionic liquid at 353 K. Potential: 3.8 V vs. Na/Na^+.

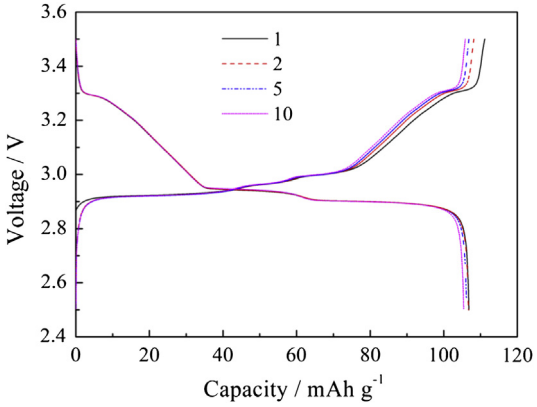

Fig. 6. Charge–discharge curves of Na/NaFSA–C_1C_3pyrFSA/$NaCrO_2$ cell at 353 K. Charge–discharge rate: 20 mA g^{-1}. Cut-off voltage: 2.5–3.5 V. Cycle number: 1, 2, 5, and 10.

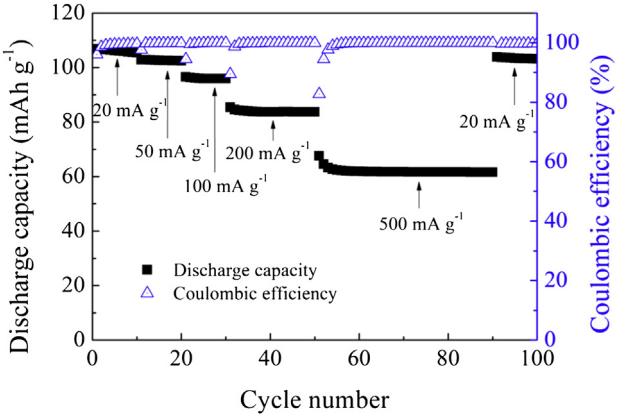

Fig. 8. Discharge capacity and coulombic efficiency for Na/NaFSA–C_1C_3pyrFSA/$NaCrO_2$ cell at 353 K. Charge–discharge rate: 20, 50, 100, 200, 500, and 20 mA g^{-1}. Cut-off voltage: 2.5–3.5 V.

363 K [21], which is explained by the formation of a passivation film on the aluminium surface [27]. The passivation film is probably formed by the reaction between Al^{3+} and FSA^- [21].

Fig. 6 shows the charge–discharge curves of a Na/NaFSA–C_1C_3pyrFSA/$NaCrO_2$ cell tested in the cell voltage range 2.5–3.5 V at a constant current of 20 mA $(g\text{-}NaCrO_2)^{-1}$ at 353 K. Potential plateaus are observed at 2.9–3.0 V in both charge and discharge curves, in addition to other potential plateaus at 3.3 V. In the first cycle, the discharge capacity and coulombic efficiency are 106 mAh $(g\text{-}NaCrO_2)^{-1}$ (close to the theoretical capacity of 125 mAh $(g\text{-}NaCrO_2)^{-1}$) and 95%, respectively. The charge–discharge tests are then conducted at higher charge–discharge rates using the same cell. Fig. 7 shows the charge–discharge curves of the Na/NaFSA–C_1C_3pyrFSA/$NaCrO_2$ cell at charge–discharge rates of 20, 50, 100, 200, 500, and 20 mA $(g\text{-}NaCrO_2)^{-1}$. The capacities gradually decrease with increasing charge–discharge rate. The shapes of the charge–discharge curves remain unchanged at the higher charge–discharge rates. After being conducted at the higher charge–discharge rate of 500 mA $(g\text{-}NaCrO_2)^{-1}$, charge–discharge test was performed again at the rate of 20 mA $(g\text{-}NaCrO_2)^{-1}$. It can be seen from Fig. 7 that the charge–discharge curve obtained for the second time at 20 mA $(g\text{-}NaCrO_2)^{-1}$ is almost the same as that obtained for the first time, except for a small decrease in capacity. This result indicates that no side reaction occurs during the cycles.

Fig. 8 shows a plot of the variations of discharge capacity and coulombic efficiency during the cycles at charge–discharge rates of 20, 50, 100, 200, 500, and 20 mA $(g\text{-}NaCrO_2)^{-1}$. The discharge capacity becomes almost constant after the initial few cycles at each charge–discharge rate. It decreases with increasing charge–discharge rate and can almost be fully recovered to the initial value when using a low charge–discharge rate. Except for the initial few cycles, the coulombic efficiency is higher than 99% at each charge–discharge rate. These results indicate that the electrolyte and electrode materials are stable at 353 K.

Fig. 9 shows the steady charge–discharge curves of the Na/NaFSA–C_1C_3pyrFSA/$NaCrO_2$ cell tested at the charge–discharge rate of 20 mA $(g\text{-}NaCrO_2)^{-1}$, at 298 and 353 K. The discharge capacity and coulombic efficiency at 353 K are 106 mAh $(g\text{-}NaCrO_2)^{-1}$ and 99.6%, respectively. The charge–discharge curves obtained at 298 K are similar to those obtained at 353 K, but the capacities decrease when the operating temperature is reduced. The discharge capacity and coulombic efficiency at 298 K are 92 mAh $(g\text{-}NaCrO_2)^{-1}$ and 99.7%, respectively. Although the discharge capacity decreases at lower temperature of 298 K, the coulombic efficiency maintains high values over 99.7%. These results indicate that the Na/NaFSA–C_1C_3pyrFSA/$NaCrO_2$ cell can be operated at room temperature as well.

From these results, it is concluded that the Na/NaFSA–C_1C_3pyrFSA/$NaCrO_2$ cell is highly promising as a new rechargeable sodium secondary battery that can operate over a wide temperature range.

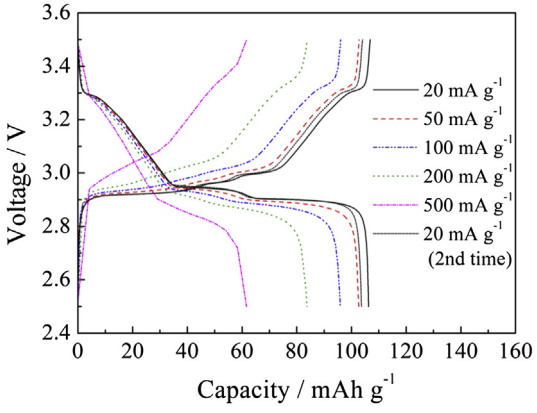

Fig. 7. Charge–discharge curves of Na/NaFSA–C_1C_3pyrFSA/$NaCrO_2$ cell at 353 K. Charge–discharge rate: 20, 50, 100, 200, and 500 mA g^{-1}. Cut-off voltage: 2.5–3.5 V.

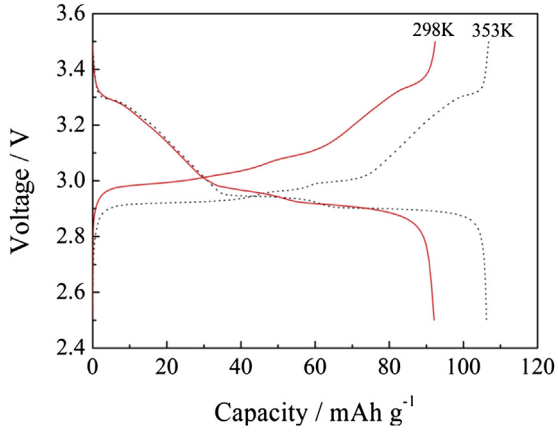

Fig. 9. Charge–discharge curves of Na/NaFSA–C_1C_3pyrFSA/$NaCrO_2$ cell at 298 and 353 K. Charge–discharge rate: 20 mA g^{-1}. Cut-off voltage: 2.5–3.5 V.

4. Conclusion

The physicochemical properties of NaFSA–C_1C_3pyrFSA ionic liquids have been investigated. The viscosity and ionic conductivity of the NaFSA–C_1C_3pyrFSA ionic liquid with a molar ratio of 2:8 at 353 K are 16.7 cP and 15.6 mS cm^{-1}, respectively. This ionic liquid exhibits a wide electrochemical window of 5.2 V at 353 K. The Na/NaFSA–C_1C_3pyrFSA/$NaCrO_2$ cell shows excellent cycle and rate performance at 353 K. The discharge capacities at 20 and 500 mA $(g\text{-}NaCrO_2)^{-1}$ are 106 and 62 mAh g^{-1}, respectively. Except for the initial few cycles, the coulombic efficiency is higher than 99% during the charge–discharge tests. The Na/NaFSA–C_1C_3pyrFSA/$NaCrO_2$ cell also shows stable charge–discharge behaviour at 298 K. The discharge capacity and coulombic efficiency at 298 K are 92 mAh $(g\text{-}NaCrO_2)^{-1}$ and 99.7%, respectively. These results indicate that the NaFSA–C_1C_3pyrFSA ionic liquid is a promising electrolyte for sodium secondary batteries operating over a wide temperature range.

Acknowledgement

This study was partly supported by a Grant-in-Aid for Scientific Research A (No. 20246140) from the Japan Society for the Promotion of Science (JSPS) and by the Advanced Low Carbon Technology Research and Development Program (ALCA) of Japan Science and Technology Agency (JST).

Appendix A. Supplementary data

Supplementary data related to this article can be found at http://dx.doi.org/10.1016/j.jpowsour.2013.03.089.

References

[1] J.M. Tarascon, M. Armand, Nature 414 (2001) 359–367.
[2] J.L. Sudworth, J. Power Sources 11 (1984) 143–154.
[3] T. Oshima, M. Kajita, A. Okuno, Int. J. Appl. Ceram. Technol. 1 (2004) 269–276.
[4] J. Coetzer, J. Power Sources 18 (1986) 377–380.
[5] C.H. Dustmann, J. Power Sources 127 (2004) 85–92.
[6] B.L. Ellis, W.R.M. Mskahnouk, Y. Makimura, K. Toghill, L.F. Nazar, Nat. Mater. 6 (2007) 749–753.
[7] I.D. Gocheva, M. Nishijima, T. Doi, S. Okada, J. Yamaki, T. Nishida, J. Power Sources 187 (2009) 247–252.
[8] N. Recham, J.N. Chotard, L. Dupont, K. Djellab, M. Armand, J.M. Tarascon, J. Electrochem. Soc. 156 (2009) A993–A999.
[9] S. Komaba, T. Nakayama, A. Ogata, T. Shimizu, C. Takei, S. Takeda, A. Hokura, N. Nakai, ECS Trans. 16 (2009) 43–55.
[10] S. Komaba, C. Takei, T. Nakayama, A. Ogata, N. Yabuuchi, Electrochem. Commun. 12 (2010) 355–358.
[11] Y. Yamada, T. Doi, I. Tanaka, S. Okada, J. Yamaki, J. Power Sources 196 (2011) 4837–4841.
[12] Y. Kawabe, N. Yabuuchi, M. Kajiyama, N. Fukuhara, T. Inamasu, R. Okuyama, I. Nakai, S. Komaba, Electrochem. Commun. 13 (2011) 1225–1228.
[13] M. Egashira, T. Tanaka, N. Yoshimoto, M. Morita, Electrochemistry 80 (2012) 755–758.
[14] N. Yabuuchi, H. Yoshida, S. Komaba, Electrochemistry 80 (2012) 716–719.
[15] S. Wenzel, T. Hara, J. Janek, P. Adelhelm, Energy Environ. Sci. 4 (2011) 3342–3345.
[16] D.H. Kim, S.H. Kang, M. Slater, S. Rood, J.T. Vaughey, N. Karan, M. Balasubramanian, C.S. Johnson, Adv. Energy Mater. 1 (2011) 333–336.
[17] V. Palomares, P. Serras, I. Villaluenga, K.B. Hueso, J.C. Gonzalez, T. Rojo, Energy Environ. Sci. 5 (2012) 5884–5901.
[18] A. Ponrouch, E. Marchante, M. Courty, J.M. Tarascon, M.R. Palacin, Energy Environ. Sci. 5 (2012) 8572–8583.
[19] L. Zhao, H.L. Pan, Y.S. Hu, H. Li, L.Q. Chen, Chin. Phys. B 21 (2012) 028201-1–028201-4.
[20] T. Nohira, T. Ishibashi, R. Hagiwara, J. Power Sources 205 (2012) 506–509.
[21] A. Fukunaga, T. Nohira, Y. Kozawa, R. Hagiwara, S. Sakai, K. Nitta, S. Inazawa, J. Power Sources 209 (2012) 52–56.
[22] Q. Zhou, W.A. Henderson, G.B. Appetecchi, M. Montanino, S. Passerini, J. Phys. Chem. B 112 (2008) 13577–13580.
[23] M. Ishikawa, T. Sugimoto, M. Kikuta, E. Ishiko, M. Kono, J. Power Sources 162 (2006) 658–662.
[24] E. Paillard, Q. Zhou, W.A. Henderson, G.B. Appetecchi, M. Montanino, S. Passerini, J. Electrochem. Soc. 156 (2009) A891–A895.
[25] X. Xia, J.R. Dahn, Electrochem. Solid-State Lett. 15 (2012) A1–A4.
[26] K. Kuratani, N. Uemura, H. Senoh, H.T. Takeshita, T. Kiyobayashi, J. Power Sources 223 (2013) 175–182.
[27] A. Watarai, K. Kubota, M. Yamagata, T. Goto, T. Nohira, R. Hagiwara, K. Ui, N. Kumagai, J. Power Sources 183 (2008) 724–729.